Supporting Information

Mesoporous TiO_2 layer suppresses ion accumulation in perovskite solar cells

Shaoshuai Miao, Shuai Yuan, Dongping Zhu, Qingbin Cai, Hao-Yi Wang, Yi Wang,* Yujun Qin* and Xi-Cheng Ai*

Key Laboratory of Advanced Light Conversion Materials and Biophotonics, Department of Chemistry, Renmin University of China, Beijing 100872, China

E-mail: ywang@ruc.edu.cn, yjqin@ruc.edu.cn, xcai@ruc.edu.cn

S1. Preparation of perovskite film and device

The FTO substrates were ultrasonically cleaned with detergent, acetone, water, and ethanol for 20 min, then dried by air gun and treated by oxygen plasma for 15 min. The SnO_2 colloidal solution (1:5 by a volume ratio with deionized water) was spin-coated on FTO substrates at 5000 rpm for 30 s and annealed on the hotplate for 30 min at 150 °C. Then TiO_2 colloidal solution (80 mg mL^{-1}) and was spin-coated on SnO_2/FTO before annealed at 500 ℃ for 4 h in a muffle furnace. For the preparation of mixed cationic perovskite film layer, PbI_2 dissolved in DMF-DMSO solvent (9:1, by volume) was spin-coated on TiO_2/SnO_2/FTO at 1500 rpm for 30 s, and annealed at 70 ℃ for 1 min. Then a solution prepared by dissolving FAI (90 mg), MABr (9 mg), and MACl (9 mg) in isopropanol (1 mL) was spin-coated on the PbI_2 films at 2000 rpm for 30 s, and then annealed at 150 ℃ for 20 min. Subsequently, the HTL solution was prepared by dissolving 72.3 mg of spiro-OMeTAD in 1 mL of CB and mixing with 28.8 mL of 4-*tert*-butylpyridine, 28.8 mL of cobalt (III) FK209/acetonitrile (300 mg mL^{-1}), and 17.5 mL of Li-TFSI/acetonitrile (520 mg mL^{-1}). The HTL solution was then spin-coated on the perovskite films at 4000 rpm for 30 s. Finally, about 80 nm Au top electrode was deposited by vacuum evaporation to form PSC devices.

S2. Characterization of films and devices

The morphology of substrates and perovskite films was characterized by field emission scanning electron microscopy (SEM, Hitachi SU8010) at 5 kV. X-ray diffraction (XRD) analysis was performed on a Shimadzu XRD-7000 diffractometer using Cu Kα radiation in the 2θ range from 10 ° to 70 ° at the scan rate of 3° per min. The UV-Vis absorption was determined by an Agilent Cary 60 spectrometer. Thermal admittance spectroscopy (TAS) measurements were performed using a Zahner PP211 with a frequency range from 0.1 to 10^6 Hz. Steady-state photoluminescence (PL) and time-resolved PL (TRPL) were conducted on an Edinburgh FLS 980 spectrometer with 475 nm laser (EPL-470, 95 ps). The space-charge-limited current (SCLC) was measured under the dark condition by the Keithley 4200 with the voltage range between

−0.1 and 1.5 V. The current density–voltage (*J*–*V*) curves were obtained by a Keithley 2400 source-meter under AM 1.5 illumination (100 mW cm^{-2}).

The OCVD and TRCE were measured by the same equipment, which consists of the light source, sample and signal collection system. The light source is provided by the continuous wave light emitting diode (LED, 520 nm, 170 μJ cm^{-2}), and controlled by the function pulse generator (Stanford Research Systems, DG535) to modulate the pulsed laser. The signal was collected by a digital oscilloscope (Lecroy, HDO4054A). The light irradiates the sample from the side of the transparent electrode, and the short circuit and open circuit are realized through two resistors (50 Ω and 1 MΩ, respectively) in series.

S3. SEM images of perovskite films with different m-TiO_2 thicknesses

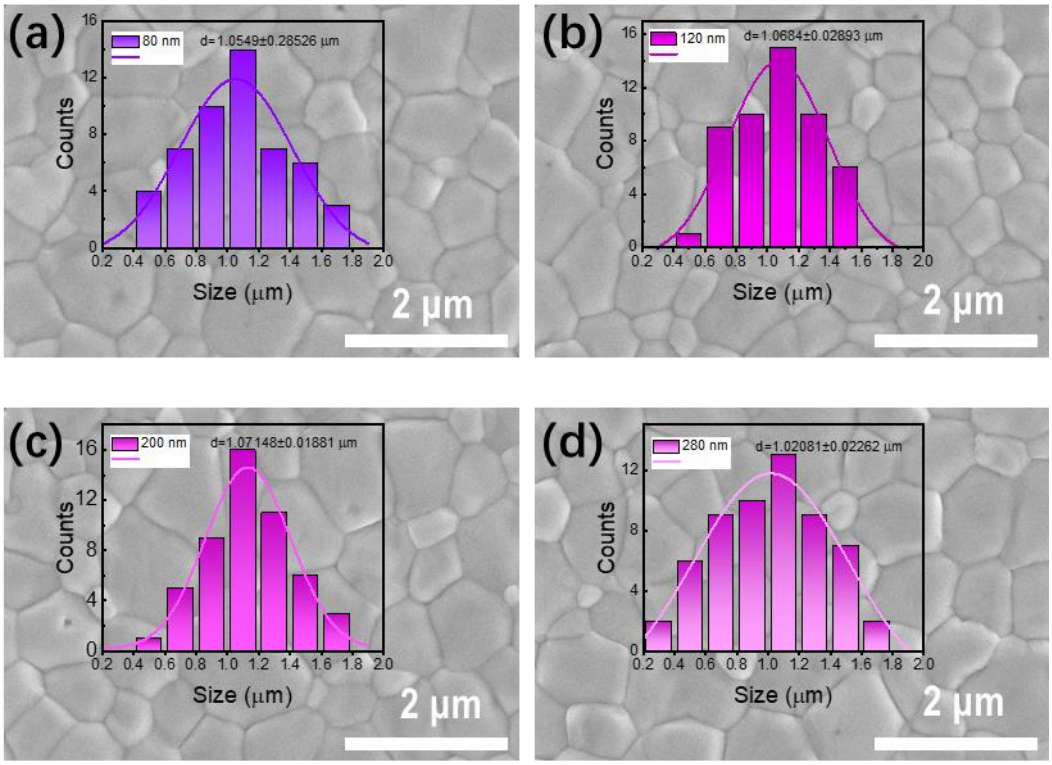

Fig. S1. Top-view SEM images of perovskite films with different m-TiO_2 thicknesses: (a) 80 nm, (b) 120 nm, (c) 200 nm, (d) 280 nm. Insets: grain size distribution of perovskite polycrystals.

S4. Fitting results of TRPL spectra

Table S1. Fitting results of the TRPL kinetics of perovskite films with different m-TiO_2 thicknesses.

Thickness	A_1	τ_1	A_2	τ_2	$<\tau>$
80 nm	0.47	107 ns	0.53	424 ns	275 ns
120 nm	0.41	69 ns	0.59	364 ns	243 ns
200 nm	0.42	60 ns	0.58	352 ns	229 ns
280 nm	0.39	55 ns	0.61	323 ns	218 ns

S5. Statistics of the photovoltaic parameters of the PSCs with different m-TiO_2 thicknesses

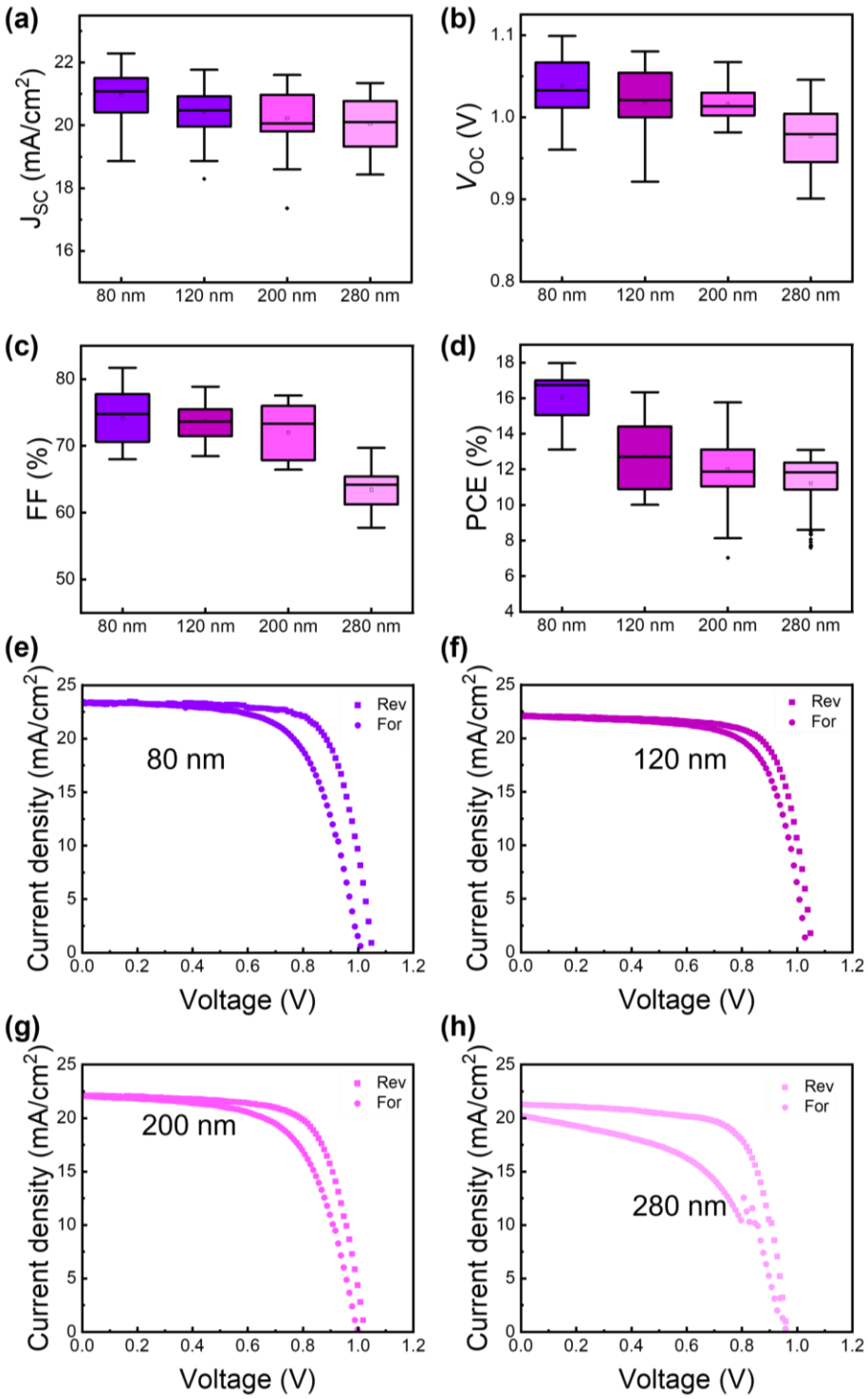

Fig. S2. Statistical photovoltaic parameters of (a) J_{SC}, (b) V_{OC}, (c) FF, (d) PCE and (e-h) typical current density-voltage curves of PSCs with different m-TiO_2 thickness.

S6. Frequency-dependent capacitance of the PSCs with different m-TiO_2 thicknesses

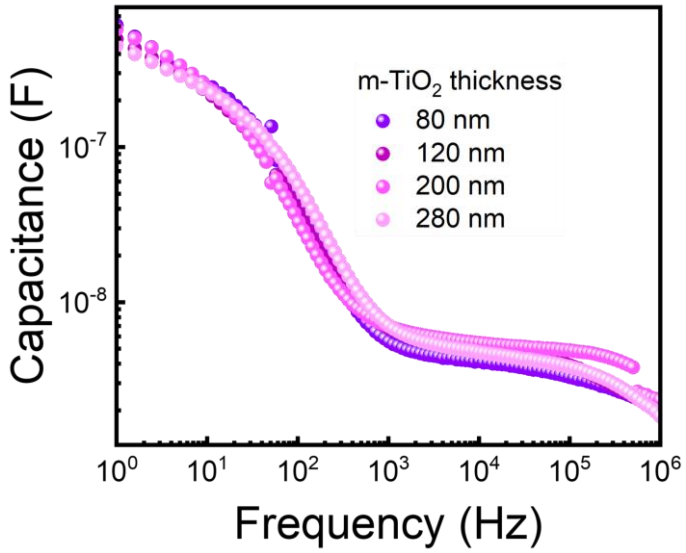

Fig. S3. *C–f* curves of PSCs with different m-TiO_2 thicknesses.

The trap density of states (*t*DOS) in perovskite solar cells can be derived from the frequency dependent capacitance characteristics with the following equation:

$$N_{\mathrm{t}}(E_{\omega}) = -\frac{V_{\mathrm{bi}}}{qW}\frac{dC}{d\omega}\frac{\omega}{k_{\mathrm{B}}T},$$

$$E_{\omega} = k_{\mathrm{B}}T\ln\left(\frac{\omega_0}{\omega}\right),$$

where W, V_{bi}, q, K_{B}, T, ω, ω_0, and C correspond to the absorption layer thickness, built-in potential, elementary charge, Boltzmann constant, temperature, angular frequency, escape angular frequency, and capacitance, respectively.[S1]

S7. The representative kinetics of the OCVD and the corresponding TRCE results for the planar and mesoporous PSCs

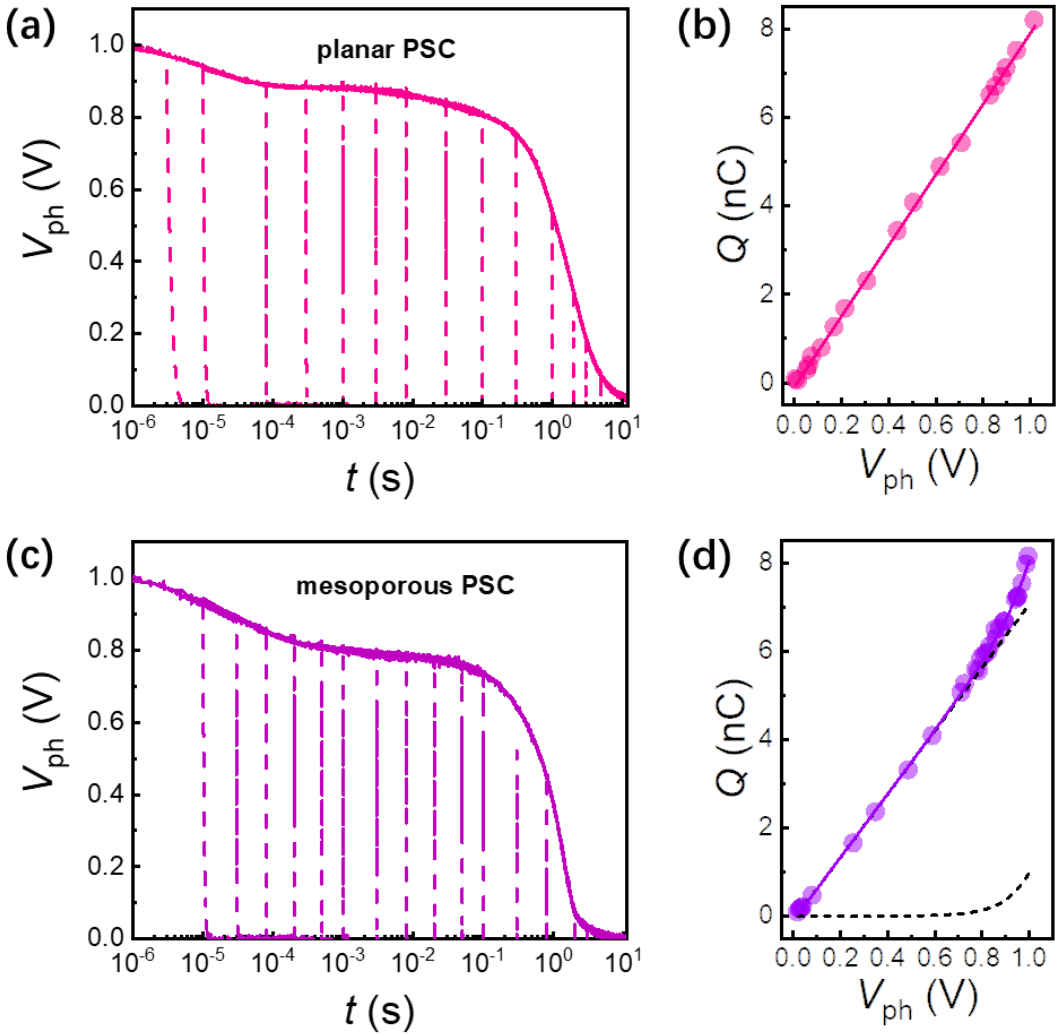

Fig. S4. Representative TRCE data of (a) planar and (c) mesoporous PSCs, where the solid curves are OCVD traces, and the dashed lines present the charge extraction procedures by abruptly switching the circuit from the open state to the short state. Q-V_{ph} plots of (b) planar and (d) mesoporous PSCs fitted with a linear function and a linear plus exponential function, respectively.

Fig. S4 shows the characteristic OCVD and TRCE results for the planar and mesoporous devices. Specifically, the solid curves and the dotted lines in Fig. S4a and S4c correspond to the voltage decay and the charge extraction processes, respectively. As detailed in the ref,[S2,3] invoking the relation between the charge amount and the photovoltage, $dQ=\int V/R\ dt$, the Q-V_{ph} plots can be obtained as shown in Fig. S4b and

S4d. Interestingly, the planar PSCs show a linear Q-V_{ph} dependence, while for the mesoporous PSCs, it shows a linear part superposed by an exponential one.

References:

S1 Z. Ni, C. Bao, Y. Liu, Q. Jiang, W. Q. Wu, S. Chen, X. Dai, B. Chen, B. Hartweg, Z. Yu, Z. Holman and J. Huang, Resolving spatial and energetic distributions of trap states in metal halide perovskite solar cells, *Science*, 2020, **367**, 1352-1358.

S2 Y. Wang, D. Wu, L. M. Fu, X. C. Ai, D. Xu and J. P. Zhang, Density of state determination of two types of intra-gap traps in dye-sensitized solar cells and its influence on device performance, *Phys. Chem. Chem. Phys.*, 2014, **16**, 11626-11632.

S3 Y. Wang, H.-Y. Wang, J. Han, M. Yu, M.-Y. Hao, Y. Qin, L.-M. Fu, J.-P. Zhang and X.-C. Ai, The Influence of Structural Configuration on Charge Accumulation, Transport, Recombination, and Hysteresis in Perovskite Solar Cells, *Energy Technol.*, 2017, **5**, 442-451.